

Inorganic Supramolecular Host Architectures: $[(M@18c6)_2][TiI_4] \cdot 2H_2O$,
 $M = 0.5 Ti, (NH_4, NH_3), (H_3O, H_2O)$

Franziska Rieger and Anja-V. Mudring*

Institut für Anorganische Chemie, Universität zu Köln, Greinstr. 6, D-50939 Köln, Germany

Received August 22, 2005

The compounds $[(M@18c6)_2][TiI_4] \cdot 2H_2O$, $M = Ti, (NH_4, NH_3), (H_3O, H_2O)$ (cubic, $F\bar{d}3$; $a = 1481.00$ pm, for $M = 0.5 Ti$, $a = 1304.65$ pm for $M = (NH_4, NH_3)$, $a = 1313.67$ pm for $M = (H_3O, H_2O)$) can be obtained from solution in the presence of traces of transition metal halides (like copper and mercury halides). Apparently the transition metal cations work as a template in the form of tetrahedral $[MX_4]$ units during the synthesis of the supramolecular host architecture. That the compounds are versatile host lattices for tetrahedrally coordinated transition metal units becomes obvious by the large group of known host–guest complex compounds, $[(M^II X_4)(M^I@18c6)_4][TiX_4]_2 \cdot nH_2O$ ($M^II = Cu, Co, Zn, Mn$; $M^I = NH_4^+, Rb, Ti$; $X = Cl, Br$).

Introduction

Concepts of supramolecular chemistry like self-assembly and crystal engineering have gained much recognition over the past years. One of the challenging areas is the design of inclusion compounds. Recently, a large structural family of supramolecular complexes with the general composition $[(M^II X_4)(M^I@18c6)_4][TiX_4]_2 \cdot nH_2O$ ($M^II = Cu, Co, Zn, Mn$; $M^I = NH_4, Rb, Ti$; $X = Cl, Br$), Figure 1, was investigated.^{1–5} This research was originally motivated by the discovery of thallium-based superconductors such as $Tl_2Ba_2Ca_2Cu_3O_{10}$ ⁶ and $Tl_2Ba_2CaCu_2O_8$ ⁷ and the increasingly important question of the environmental disposition of (toxic) thallium by extraction or immobilization applying supramolecular concepts. Indeed, thallium can be chemically bound in the form of $[TiI_4]^-$ anions by a combined oxidation/complexation process.^{1–5}

* To whom correspondence should be addressed. E-mail: a.mudring@uni-koeln.de.

- (1) Kahwa, I. A.; Miller, D.; Mitchell, M.; Fronczek, F. R.; Goodrich, R. G.; Williams, D. J.; O'Mahoney, C. A.; Slawin, A. M. Z.; Ley, S. V.; Groombridge, C. J. *Inorg. Chem.* **1992**, *31*, 3963.
- (2) Kahwa, I. A.; Miller, D.; Mitchell, M.; Fronczek, F. R. *Acta Crystallogr. C* **1993**, *49*, 320.
- (3) Fender, N. S.; Finnegan, S. A.; Miller, D.; Mitchell, M.; Kahwa, I. A.; Fronczek, F. R. *Inorg. Chem.* **1994**, *33*, 4002.
- (4) Fender, N. S.; Fronczek, F. R.; John, V.; Kahwa, I. A.; McPherson, G. L. *Inorg. Chem.* **1997**, *36*, 5539.
- (5) Fender, N. S.; Kahwa, I. A.; Fronczek, F. R. *J. Solid State Chem.* **2002**, *163*, 286.
- (6) Torardi, C. C.; Subramanian, M. A.; Calabrese, J. C.; Gopalakrishnan, J.; Morrissey, K. J.; Askew, R. R.; Flippen, R. B.; Chowdhry, U.; Sleight, A. W. *Science* **1988**, *240*, 631.
- (7) Subramanian, M. A.; Calabrese, J. C.; Torardi, C. C.; Gopalakrishnan, J.; Askew, R. R.; Flippen, R. B.; Morrissey, K. J.; Chowdhry, U.; Sleight, A. W. *Nature* **1988**, *332*, 420.

The resulting compounds with the general composition $[(M^II X_4)(M^I@18c6)_4][TiX_4]_2$ contain tetrahedral transition metal units, $[M^II X_4]^{2-}$, incorporated in a complex cubic framework. The first coordination shell of $[M^II X_4]^{2-}$ is formed by a tetrahedron of four $[M@18c6]$ units while an adamantane-like grouping of 10 $[TiX_4^-]$ units forms the second shell (cf. Figure 1). Subject to their structure these compounds have been addressed as “double-shell lattice clathrates”;⁸ although we believe that the class of compounds under discussion cannot be regarded as true clathrate compounds as they do not show the features which are characteristic for clathrate compounds, for example the “included” tetrahedral transition metal units $[M^II X_4]^{2-}$ cannot be removed without any deprotonation or ion-exchange process in the host lattice. Here, we report on three *guest-free* host structures, $[(M@18c6)_2][TiI_4] \cdot 2H_2O$ with $M = (H_3O, H_2O), (NH_4, NH_3)$, and Ti , showing that the structures can exist without the inner transition metal tetrahedron and thus are true host structures.

Experimental Section

Materials. Thallium iodide (99.9%, Aldrich), 18-crown-6 (>98%, Merck), iodine (99.8%, Riedel-de Haën), ammonium iodide (99.5%, Merck), copper(I)iodide (>98%, Merck), acetonitrile (99.5%, Merck), and hydroiodic acid (57 wt.-%, Merck) were used.

Syntheses. The respective reactants are placed in 20 mL of acetonitrile, heated under stirring to 70 °C until the bulk is dissolved and a dark red solution is obtained. Quasi-isothermal evaporation

- (8) Domasevitch, K. V.; Rusanova, J. A.; Sieler, J.; Kokozay, V. N. *Inorg. Chim. Acta* **1999**, *293*, 234.

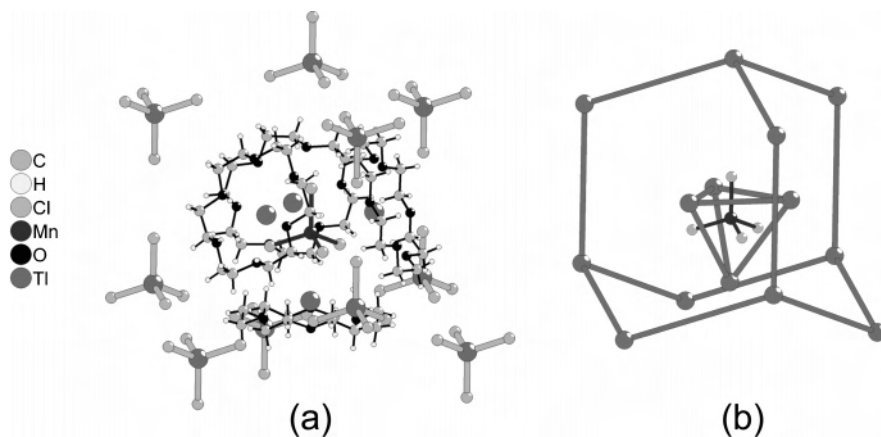


Figure 1. Part of the crystal structure of $[(\text{MnCl}_4)(\text{Tl}@18\text{c}6)_4][\text{TlCl}_4]_2$ (ref 3) illustrating the double-shell nature of $[(\text{M}^{\text{II}}\text{X}_4)(\text{M}^{\text{I}}@18\text{c}6)_4][\text{TlX}_4]_2 \cdot n\text{H}_2\text{O}$ -type compounds. The inner $[\text{MnCl}_4]^-$ tetrahedron is surrounded tetrahedrally by four $\text{Tl}@18\text{c}6$ units, an outer adamantane-like shell of 10 $[\text{TlCl}_4]^-$ tetrahedra wraps around this unit. In panel a, all atoms are present, and in panel b, the chloride atoms and crown ether molecules are omitted for clarity. The thallium cations are connected by grey lines to demonstrate the building scheme.

yields, after 3 days, in all cases, ruby red crystals, which are isolated from the solution. As dry $[(\text{H}_3\text{O},\text{H}_2\text{O})@(\text{18c}6)_2][\text{TlI}_4] \cdot 2\text{H}_2\text{O}$ decomposes when exposed to air all manipulations for further analysis were carried out under an inert atmosphere.

$[\text{Tl}@(\text{18c}6)_2][\text{TlI}_4] \cdot 2\text{H}_2\text{O}$. Thallium(I) iodide (33.7 mg, 0.102 mmol), 18-crown-6 (55.0 mg, 0.208 mmol), copper(I) iodide (1.4 mg, 0.0074 mmol), and iodine (39.2 mg, 0.307 mmol) were used.

$[(\text{NH}_4,\text{NH}_3)@(\text{18c}6)_2][\text{TlI}_4] \cdot 2\text{H}_2\text{O}$. Ammonium iodide (9.2 mg, 0.063 mmol), thallium(I) iodide (18.6 mg, 0.0561 mmol), copper(I) iodide (1.4 mg, 0.0074 mmol), 18-crown-6 (55.0 mg, 0.208 mmol), and iodine (38.1 mg, 0.300 mmol) were used.

$(\text{H}_3\text{O},\text{H}_2\text{O})@(\text{18c}6)_2][\text{TlI}_4] \cdot 2\text{H}_2\text{O}$. Thallium(I) iodide (33.1 mg, 0.100 mmol), 18-crown-6 (52.8 mg, 0.200 mmol), copper(I) iodide (1.4 mg, 0.0074 mmol), iodine (39.2 mg, 0.298 mmol), and hydroiodic acid (0.1 mL, 57 wt. %) were used.

Vibrational Spectroscopy/Infrared Spectra. $[\text{Tl}@(\text{18c}6)_2][\text{TlI}_4] \cdot 2\text{H}_2\text{O}$: 3436.6 (m), 3005.9 (w), 2885.8 (s), 2818.3 (w), 2736.7 (w), 2283.9 (w), 2242.1 (w), 1972.1 (w), 1633.3 (w), 1478.6 (m), 1452.6 (m), 1429.8 (w), 1347.4 (m), 1280.4 (m), 1244.4 (m), 1231.7 (w), 1111.8 (s), 1053.0 (s), 961.5 (s), 837.8 (m), 150.2 (m), 51.0 cm^{-1} (w).

$[(\text{NH}_4,\text{NH}_3)@(\text{18c}6)_2][\text{TlI}_4] \cdot 2 \text{H}_2\text{O}$: 3441.4 (m), 3198 (m), 2941.7 (w), 2887.3 (s), 2821.8 (w), 2739.4 (w), 2286.1 (w), 2245.7 (w), 1971.9 (w), 1479.2 (m), 1453.5 (m), 1428.7 (m), 1347.9 (m), 1280.0 (m), 1245.3 (m), 1232.4 (m), 1112.3 (s), 1053.2 (m), 962.4 (s), 838.9, 150.2 (s), 52.9 cm^{-1} (w).

$(\text{H}_3\text{O},\text{H}_2\text{O})@(\text{18c}6)_2][\text{TlI}_4] \cdot 2\text{H}_2\text{O}$: 3438.2 (m), 3197.1 (m), 2877.7 (w), 2817.3 (s), 2817.8 (m), 2286.1 (w), 2244.6 (w), 1974.4 (w), 1748.0 (w), 1720.1 (m), 1632.0 (m), 1473.5 (m), 1452.2 (m), 1429.9 (m), 1347.7 (s), 1281.0 (m), 1244.9 (m), 1232.0 (m), 1112.6 (s), 1054.7 (m), 960.5 (s), 838.8 (m), 149.0 (s), 51.0 cm^{-1} (w).

Powder X-ray Diffraction. Powder X-ray diffraction data were obtained using a Stoe Stadip diffractometer (Cu $\text{K}\alpha_1$, image plate).

$[\text{Tl}@(\text{18c}6)_2][\text{TlI}_4] \cdot 2 \text{H}_2\text{O}$: cubic, $a = 2130.5(8)$ pm (Cu $\text{K}\alpha_1$, 293 K, 38 indexed lines), Figure 2.

$[(\text{NH}_4,\text{NH}_3)@(\text{18c}6)_2][\text{TlI}_4] \cdot 2 \text{H}_2\text{O}$: cubic, $a = 2134.3(3)$ pm (Cu $\text{K}\alpha_1$, 293 K, 38 indexed lines), Figure 3.

$(\text{H}_3\text{O},\text{H}_2\text{O})@(\text{18c}6)_2][\text{TlI}_4] \cdot 2 \text{H}_2\text{O}$: cubic, $a = 2132.0(3)$ pm (Cu $\text{K}\alpha_1$, 293 K, 51 indexed lines), Figure 4.

Elemental analysis (C,H,N). $[\text{Tl}@(\text{18c}6)_2][\text{TlI}_4] \cdot 2 \text{H}_2\text{O}$. Found: 22.9, C; 0.2, N; 3.6, H. Calcd: 19.4, C; 3.5, H.

$[(\text{NH}_4,\text{NH}_3)@(\text{18c}6)_2][\text{TlI}_4] \cdot 2 \text{H}_2\text{O}$. Found: 22.5, C; 2.1, N; 4.2, H. Calcd: 22.0, C; 2.1, N; 4.5, H.

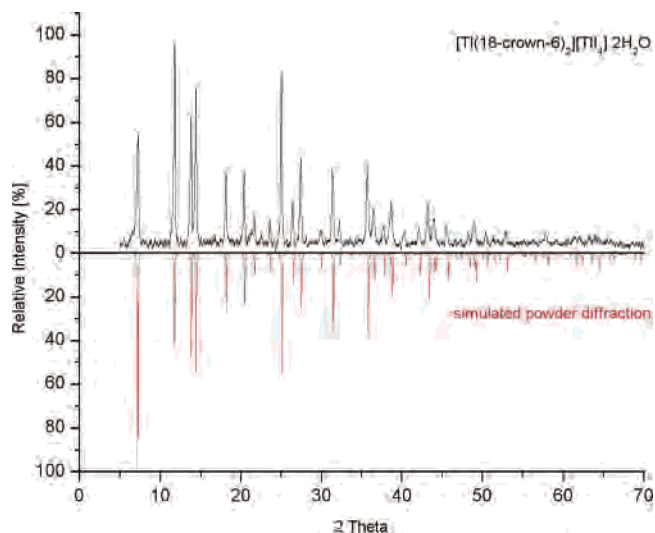


Figure 2. X-ray powder diffraction pattern of $[\text{Tl}@(\text{18c}6)_2][\text{TlI}_4] \cdot 2\text{H}_2\text{O}$: (black) measured data and (red) pattern simulated from single-crystal data.

$(\text{H}_3\text{O},\text{H}_2\text{O})@(\text{18c}6)_2][\text{TlI}_4] \cdot 2 \text{H}_2\text{O}$. Found: 22.3, C; 0.1, N; 4.4, H. Calcd: 22.3, C; 4.4, H.

Crystal Structure Determinations. A few crystals of each compound were selected and sealed in thin-walled glass capillaries of 0.1–0.3 mm outer diameter and were checked by Laue photographs for their quality. The best specimen was used to collect a complete intensity data set with the aid of a single-crystal X-ray diffractometer (Stoe IPDS II, graphite-monochromated Mo $\text{K}\alpha$ X-ray radiation, $\lambda = 0.70173 \text{ \AA}$). Essential experimental conditions and the resulting crystallographic data are summarized in Table 1. Fractional atomic coordinates and isotropic displacement factors are given in Table 2. For interatomic distances see Table 4, and for complete data see the CIF file (Supporting Information). Data reduction with the program X-Red⁹ in all cases included corrections for background and Lorentz and polarization effects. A numerical absorption correction with the programs X-Red/X-Shape⁹ was undertaken after optimization of the habitus of the crystal. All compounds crystallize in the cubic space group $Fd\bar{3}$ (No. 203). The structures were solved by direct methods with the program SHELXS-97.¹⁰ Non-hydrogen atoms were refined anisotropically

(9) X-RED, X-Shape; Stoe & Cie: Darmstadt, Germany, 2002.

(10) Sheldrick, W. S. SHELXS-97; Universität Göttingen: Göttingen, Germany, 1997.

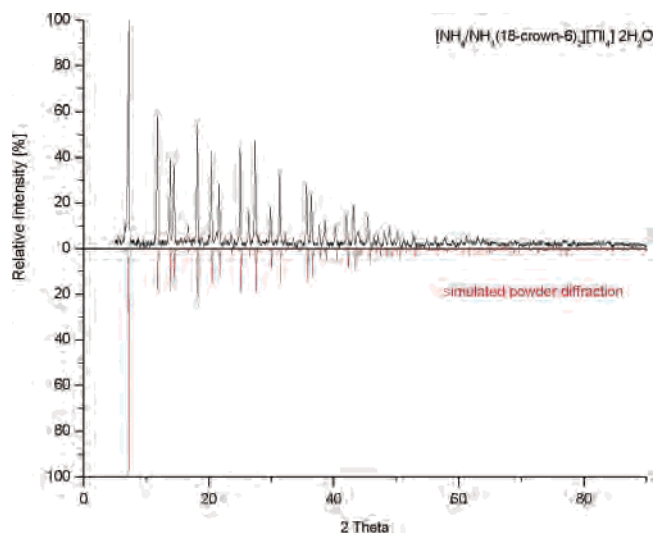


Figure 3. X-ray powder diffraction pattern for $[(\text{NH}_4,\text{NH}_3)@(18\text{c}6)_2][\text{TlI}_4] \cdot 2\text{H}_2\text{O}$: (black) measured data and (red) pattern simulated from single-crystal data.

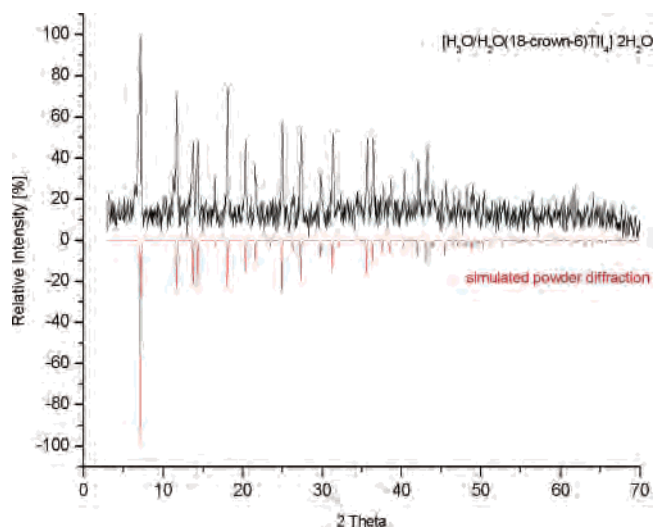


Figure 4. X-ray powder diffraction pattern for $(\text{H}_3\text{O}/\text{H}_2\text{O})@(18\text{c}6)_2[\text{TlI}_4] \cdot 2\text{H}_2\text{O}$: (black) measured data and (red) pattern simulated from single-crystal data.

by a full-matrix least-squares procedure using the program SHELXL-97.¹¹ Structure factors are taken from the International Tables for Crystallography.¹² Common isotropic thermal parameters were assigned for the hydrogen atoms. The hydrogen atoms were idealized and allowed to ride on the parent atoms. For crystal structure drawings, the program Diamond was used.¹³

Results and Discussion

The $[(\text{M}@18\text{c}6)_2][\text{TlI}_4] \cdot 2\text{H}_2\text{O}$, $\text{M} = (\text{H}_3\text{O}, \text{H}_2\text{O})$, $(\text{NH}_4, \text{NH}_3)$, and Tl , compounds crystallize in the cubic space group $Fd\bar{3}$ (No. 203) (Table 1). The common structural features are tetrahedral $[\text{TlI}_4]^-$ units with thallium–iodine distances of $d(\text{Tl}–\text{I}) = 276$ pm (Figure 5a), which are typical for tetraiodo thallates(III), as for example in CsTlI_4

($\bar{d}(\text{Tl}–\text{I}) = 275$ pm).¹⁵ The $\text{I}–\text{Tl}–\text{I}$ angle in these structures is by symmetry ideally tetrahedral, $\angle(\text{I}–\text{Tl}–\text{I}) = 109.5^\circ$. These $[\text{TlI}_4]^-$ units build up a diamond-like network (Figure 5b). A second independent diamond-like network is produced by the centers of gravity of four crown ether molecules (cf. Figure 5b). Together with the $\text{Tl}(\text{III})$ positions a network of two interpenetrating diamond nets is generated, as in NaTl .¹⁴ The crown ether molecules build by themselves a framework of corner-sharing tetrahedra comparable to those found in MgCu_2 ¹⁶ (Figure 5c). Thus, this class of compounds can be understood as decorated NaTl or MgCu_2 structures (cf. Figure 5).

In the host–guest structures of $[(\text{M}^{\text{II}}\text{X}_4)(\text{M}^{\text{I}}@18\text{c}6)_4][\text{TlX}_4]_2 \cdot n\text{H}_2\text{O}$ ($\text{M}^{\text{II}} = \text{Cu}, \text{Co}, \text{Zn}, \text{Mn}$; $\text{M}^{\text{I}} = \text{NH}_4^+, \text{Rb}, \text{Tl}$; $\text{X} = \text{Cl}, \text{Br}$) exactly one-half of the tetrahedral cavities spanned by the crown ether molecules are filled in an ordered fashion by $\text{M}^{\text{II}}\text{X}_4$ units. By this the centrosymmetry is destroyed, and the space group symmetry reduced from $Fd\bar{3}$ to $F23$. It should be emphasized that there is no need to describe the structure of the guest-free host in the noncentrosymmetric space group as it was previously reported for “ $\text{NH}_4\text{TlI}_4 \cdot 2(18\text{c}6) \cdot \text{NH}_3$ ” with the space group $F23$.⁸ Table 3 gives the transformed coordinates in the centric space group $Fd\bar{3}$ for easier comparison with our data.

The crown ether molecules, 18c6, in $[(\text{M}@18\text{c}6)_2][\text{TlI}_4] \cdot 2\text{H}_2\text{O}$, $\text{M} = (\text{H}_3\text{O}, \text{H}_2\text{O})$, $(\text{NH}_4, \text{NH}_3)$, and Tl , have crystallographic C_3 symmetry and exist in the pseudo- D_{3d} conformation with the conventional all-gauche conformations typical for this ligand in metal ion complexes¹⁷ and in the free crown ether itself.¹⁸ The $\text{C}–\text{C}$ and $\text{O}–\text{C}$ bonding distances within the crown ether found in the empty guest structures $[(\text{M}@18\text{c}6)_2][\text{TlI}_4] \cdot 2\text{H}_2\text{O}$, $\text{M} = (\text{H}_3\text{O}, \text{H}_2\text{O})$, $(\text{NH}_4, \text{NH}_3)$, and Tl (Table 3), are closely related to the values observed for the free crown ether ($\bar{d}(\text{C}–\text{C}) = 151$ pm, $\bar{d}(\text{C}–\text{O}) = 142$ pm)¹⁸ and to those of the host–guest complexes $[(\text{M}^{\text{II}}\text{X}_4)(\text{M}^{\text{I}}@18\text{c}6)_4][\text{TlI}_4]_2 \cdot n\text{H}_2\text{O}$ ($\text{M}^{\text{II}} = \text{Cu}, \text{Co}, \text{Zn}, \text{Mn}$; $\text{M}^{\text{I}} = \text{NH}_4^+, \text{Rb}, \text{Tl}$; $\text{X} = \text{Cl}, \text{Br}$).^{1–5} The $\angle(\text{C}–\text{O}–\text{C})$ and $\angle(\text{O}–\text{C}–\text{C})$ angles, which range from 112.4 to 112.7° and from 107.7 to 108.7° in the compounds under investigation, are on the average a bit smaller than in the free crown ether ($\angle(\text{C}–\text{O}–\text{C}) = 112.8^\circ$ and $\angle(\text{O}–\text{C}–\text{C}) = 109.4^\circ$, mean values) and the stuffed host–guest structures.

The values that differ most from the free crown ether and are very characteristic for complex formation are the torsion angles. The values found for $[(\text{M}@18\text{c}6)_2][\text{TlI}_4] \cdot 2\text{H}_2\text{O}$, $\text{M} = (\text{H}_3\text{O}, \text{H}_2\text{O})$, $(\text{NH}_4, \text{NH}_3)$, and Tl , are, indeed, more comparable to those found for the hydrate, $18\text{c}6 \cdot \text{H}_2\text{O}$,¹⁹ than to those found for the free crown ether. The torsional angles average within the standard deviation to be nearly the same

(14) Zintl, E.; Dullenkopf, W. *Z. Phys. Chem. B* **1932**, *16*, 195.

(15) Thiele, G.; Rotter, H. W.; Zimmermann, K. *Z. Naturforsch. B* **1986**, *41*, 269.

(16) Lieser, K. H.; Witte, H. *Z. Metallkd.* **1952**, *43*, 396.

(17) (a) Pederson, C. J. *J. Am. Chem. Soc.* **1967**, *89*, 7017. (b) Pederson, C. J.; Frensdorff, H. K. *Angew. Chem., Int. Ed. Engl.* **1971**, *11*, 16.

(18) Dunitz, J. D.; Dobler, M.; Seiler, P.; Phizackerley, R. P. *Acta Crystallogr. B* **1974**, *30*, 2733.

(19) Albert, A.; Mootz, D. *Z. Naturforsch. B* **1997**, *52*, 615.

(11) Sheldrick, W. S. *SHELXL-97*; Universität Göttingen: Göttingen, Germany, 1997.

(12) Prince, E., Ed., *International Tables for Crystallography*, Vol. C; Kluwer Academic Publishers: Dordrecht, The Netherlands, 2004.

(13) *Diamond*, version 2.1; Crystal Impact GbR: Bonn, Germany, 1998.

Table 1. Crystallographic Information for [(M@18c6)₂][TiI₄]₂·2H₂O, M = (H₃O, H₂O), (NH₄,NH₃), and TI

empirical formula	[TI@18c6) ₂][TiI ₄] ₂ ·2H ₂ O	[(NH ₄ ,NH ₃)@18c6) ₂][TiI ₄] ₂ ·2H ₂ O	[(H ₃ O,H ₂ O)@18c6) ₂][TiI ₄] ₂ ·2H ₂ O
fw	1481.00	1304.65	1313.67
temp	293(2) K	77 K	293(2) K
wavelength	71.073 pm	71.073 pm	71.073 pm
cryst syst, space group	cubic, Fd $\bar{3}$	cubic, Fd $\bar{3}$	cubic, Fd $\bar{3}$
unit cell dimensions	$a = b = c = 2122.81(13)$ pm	$a = b = c = 2123.06(16)$ pm	$a = b = c = 2137.90(18)$ pm
vol	9566.1(10) Å ³	9569.4(12) Å ³	9771.5(14) Å ³
Z, density _{calcd}	8, 2.057 mg/m ³	8, 1.811 mg/m ³	8, 1.768 mg/m ³
abs coeff	9.357 mm ⁻¹	6.004 mm ⁻¹	5.883 mm ⁻¹
F(000)	5456	4920	4976
cryst size	0.1 × 0.1 × 0.1 mm	0.1 × 0.1 × 0.1 mm	0.1 × 0.1 × 0.1 mm
θ range for data collection	1.67–25.00°	1.67–25.00°	2.69–24.95°
limiting indices	–25 < h < 25 –25 < k < 25 –25 < l < 25	–25 < h < 25 –25 < k < 25 –25 < l < 25	–25 < h < 25 –25 < k < 25 –25 < l < 25
feIfls collected/unique	28737/713 [R(int) = 0.0561]	21554/713 [R(int) = 0.0408]	21045/725 [R(int) = 0.1118]
completeness to θ = 24.98	100.0%	100.0%	99.9%
abs correction	numerical	numerical	numerical
min/max transmission	0.1575, 0.3244	0.2431, 0.4843	0.2064, 0.3401
refinement method	full-matrix least-squares on F ²	full-matrix least-squares on F ²	full-matrix least-squares on F ²
data/restraints/parameters	703/0/43	713/0/43	725/0/37
GOF on F ²	1.250	1.150	0.967
Final R indices [I > 2σ(I)]	R1 = 0.0274 wR2 = 0.0787	R1 = 0.0244 wR2 = 0.0707	R1 = 0.0361 wR2 = 0.0892
R indices (all data)	R1 = 0.0280 wR2 = 0.0790	R1 = 0.0276 wR2 = 0.0715	R1 = 0.0544 wR2 = 0.0935
extinction coeff	0.00024(2)	0.000095(17)	0.00005(2)
largest diff. peak and hole	1.267 and –0.808 e Å ⁻³	1.073 and –0.412 e Å ⁻³	0.881 and –0.710 e Å ⁻³

(Table 4). The ∠O–C–C–O angles in the empty guest structures are generally a little smaller than the average ∠O–C–C–O angles found in the host–guest structures, while the ∠C–O–C–C angles tend to be a little larger. The origin of this small deviation can be seen in the interaction of the crown ether molecules with the transition metal tetrahedra in the host–guest structures.

All M [(H₃O,H₂O), (NH₄,NH₃), TI] units of the guest free compound that are coordinated by the crown ether are located on Wyckoff position 32e and are disordered above and below the crown ether with occupancies of 0.25 for the TI, 0.5 for the (NH₄,NH₃), and 1 for the (H₃O,H₂O) compound.

For [(NH₄/NH₃)@18c6)₂][TiI₄]₂·2H₂O (Figure 6), the interatomic distance of N to the closest triangle of the crown ether oxygen atoms is $d(\text{N}–\text{O}1) = 305.8$ pm. This distance is larger than observed in, for example, [NH₄@18c6]Cl²⁰ ($d(\text{N}–\text{O}) = 290–291$ pm) but equal to that found, for example, in [(NH₄)(18c6)₂][UCl₆]₂·2CH₃CN²¹ and is the same value as that reported by Domasevitch et al.⁸ The N atoms are displaced by 138.6 pm from the mean plane of the six macrocyclic oxygen atoms (cf. [NH₄@18c6]Cl²⁰ 107 pm; [(NH₄)(18c6)₂][UCl₆]₂·2CH₃CN²¹ 99 pm). In the host–guest complexes [(NH₄(18c6)₄)MnX₄][TiX₄], X = Cl and Br,⁵ values of about $d = 132$ pm are found.

Half of the crown ether molecules in [(NH₄,NH₃)@18c6)₂][TiI₄]₂·2H₂O must coordinate to ammonia, NH₃, and the other half coordinate to ammonium, NH₄⁺, to balance the anionic counter charge. A crystal water oxygen atom (O2) resides 203.2 pm from the center of the crown ether forming hydrogen bonds to NH₃/NH₄⁺ with an N–O distance of 324–

(1) pm. The distance is at the upper limit observed for N–O hydrogen-bonding systems.²² O2 is not only involved in hydrogen bonding with NH₃/NH₄⁺ but also forms a hydrogen bond to a second water molecule (O3) with an O–O distance of $d(\text{O}2–\text{O}3) = 279(1)$ pm. As a result, two crystal water molecules are found per [(NH₄,NH₃)@18c6)₂][TiI₄]₂·2H₂O formula unit. The nitrogen (N) and crystal water oxygen positions (O2 and O3) together form a distorted cube (Figure 6b). Four crown ether molecules reside in a tetrahedron fashion above the four corners of the cube. According to the fractional occupancies of the N, O2, and O3 positions, each crown ether molecule is coordinated on one side by ammonium or ammonia and on the other side by water.

As the ammonium ion is too large to fit into the cavity of 18-crown-6, no electron density is found inside the ring in [(NH₄⁺,NH₃)@18c6)₂][TiI₄]₂·2H₂O. Most probably, the ammonium ion forms a “perching” complex, resting above the mean plane defined by the oxygen atoms of the crown ether and forming three well-directed hydrogen bonds to alternate crown ether oxygen atoms.^{23,24}

The (H₃O⁺,H₂O) compound shows basically the same structural features. The small difference between [(NH₄,NH₃)@18c6)₂][TiI₄]₂·2H₂O and [(H₃O,H₂O)@18c6)₂][TiI₄]₂·2H₂O is that N1, O2, and O3 are substituted by just one oxygen position (O2) with a larger displacement factor. Interestingly, so far no filled host–guest structures have been reported for the (H₃O,H₂O) structures.

The complexation of (NH₄⁺,NH₃) and (H₃O⁺,H₂O) by the crown ether is presumed to be mostly affected by hydrogen

(20) Pears, D. A.; Stoddart, J. F.; Fakley, M. E. *Acta Crystallogr. C* **1988**, *44*, 1426.

(21) Rogers, R. D.; Benning, M. M. *Acta Crystallogr. C* **1988**, *44*, 1397.

(22) Steiner, T. *Angew. Chem.* **2002**, *114*, 50.

(23) Bokare, A. D.; Patnaik, A. *Cryst. Res. Technol.* **2004**, *39*, 465.

(24) Steed, J. W.; Atwood, J. L. *Supramolecular Chemistry*; Wiley: New York, 2000.

Table 2. Atomic and Wyckoff Positions, Occupancy, Fractional Coordinates, and Isotropic Displacement Factors for $[(M@18c6)_2][TiL_4] \cdot 2H_2O$, $M = (H_3O, H_2O), (NH_4, NH_3)$, and Tl

[Ti@18c6 ₂][TiL ₄]·2 H ₂ O						
Wyckoff	occupancy	<i>x/a</i>	<i>y/b</i>	<i>z/c</i>	<i>U</i> _{eq}	
Tl1	8 <i>a</i>	1	1/8	1/8	1/8	23.6(3)
I	32 <i>e</i>	1	0.0500(2)	0.0500(2)	0.0500(2)	34(1)
O1	96 <i>g</i>	1	0.4016(2)	0.0842(2)	0.0308(2)	45(1)
C1	96 <i>g</i>	1	0.3791(3)	0.1190(3)	-0.0213(3)	48(2)
H11	96 <i>g</i>	1	0.3507	0.1518	-0.0071	51 (10)
H12	96 <i>g</i>	1	0.3563	0.0915	-0.0498	51 (10)
C2	96 <i>g</i>	1	0.4345(3)	0.1478(3)	-0.0547(3)	49(2)
H12	96 <i>g</i>	1	0.4200	0.1776	-0.0861	51(10)
H13	96 <i>g</i>	1	0.4610	0.1699	-0.0248	51 (10)
Tl2	32 <i>e</i>	1/4	0.46339(6)	0.46339(6)	0.46339(6)	39.0(4)
O3	32 <i>e</i>	1/4	0.4427(13)	0.4427(13)	0.4427(13)	84(16)
O4	32 <i>e</i>	1/4	0.4360(9)	0.4360(9)	0.4360(9)	104(18)
[(NH ₄ ,NH ₃)@18c6 ₂][TiL ₄]·2 H ₂ O						
Wyckoff	occupancy	<i>x/a</i>	<i>y/b</i>	<i>z/c</i>	<i>U</i> _{eq}	
Tl	8 <i>a</i>	1	1/8	1/8	1/8	25(1)
I	32 <i>e</i>	1	0.0500(1)	0.0500(1)	0.0500(1)	35(1)
O1	96 <i>g</i>	1	0.4017(2)	0.0846(2)	0.0308(2)	46(1)
C1	96 <i>g</i>	1	0.3792(3)	0.1191(3)	-0.0216(3)	51(2)
H1A	96 <i>g</i>	1	0.3506	0.1519	-0.0076	48(9)
H1B	96 <i>g</i>	1	0.3566	0.0914	-0.0500	48(9)
C2	96 <i>g</i>	1	0.4346(4)	0.1481(4)	-0.0551(4)	50(2)
H2A	96 <i>g</i>	1	0.4201	0.1779	-0.0865	48(9)
H2B	96 <i>g</i>	1	0.4612	0.1702	-0.0253	48(9)
N	32 <i>e</i>	1/2	0.4623(5)	0.4623(5)	0.4623(5)	24(4)
O2	32 <i>e</i>	1/4	0.4447(7)	0.4447(7)	0.4447(7)	46(11)
O3	32 <i>e</i>	1/4	0.4361(8)	0.4361(8)	0.4361(8)	97(15)
[(H ₃ O,H ₂ O)@18c6 ₂][TiL ₄]·2 H ₂ O						
Wyckoff	occupancy	<i>x/a</i>	<i>y/b</i>	<i>z/c</i>	<i>U</i> _{eq}	
Tl	8 <i>a</i>	1	1/8	1/8	1/8	36(1)
I	32 <i>e</i>	1	0.0504(1)	0.0504(1)	0.0504(1)	59(1)
O1	96 <i>g</i>	1	0.4155(4)	0.0978(3)	-0.315(3)	80(2)
C1	96 <i>g</i>	1	0.3819(6)	0.1200(5)	0.0205(5)	89(4)
H1A	96 <i>g</i>	1	0.3495	0.1487	0.0069	107
H1B	96 <i>g</i>	1	0.4097	0.1421	0.0487	107
C2	96 <i>g</i>	1	0.4464(5)	0.1471(5)	-0.0650(6)	86(4)
H2A	96 <i>g</i>	1	0.4763	0.1680	-0.0381	104
H2B	96 <i>g</i>	1	0.4162	0.1777	-0.0794	104
O2	32 <i>e</i>	1	0.4613(5)	0.4613(5)	0.4613(5)	105(5)

Table 3. Atomic Positions for $NH_4TiL_4 \cdot 2(18c6) \cdot NH_3$ as Reported by Domasevitch et al.⁸ after Transformation to the Centric Space Group $Fd\bar{3}$

atom	Wyckoff position	fractional coordinates		
Tl	8 <i>a</i>	1/8	1/8	1/8
I	32 <i>e</i>	0.05013	0.05013	0.05013
O1	96 <i>g</i>	0.40260	0.03305	0.08425
C1	96 <i>g</i>	0.38280	-0.02140	0.11615
H11	96 <i>g</i>	0.35080	-0.01170	0.14635
H12	96 <i>g</i>	0.36490	-0.04965	0.08610
C2	96 <i>g</i>	0.35250	0.06515	0.05375
H21	96 <i>g</i>	0.32960	0.03875	0.02560
H22	96 <i>g</i>	0.32450	0.08135	0.08480
N	32 <i>e</i>	0.46100	0.46100	0.46100
H3	16 <i>d</i>	1/2	1/2	1/2

bonding. In contrast, charge–dipole interactions are held responsible for the complexation of simple metal cations, as is the case for thallium in $[Ti(18c6)_2][TiL_4] \cdot 2H_2O$. Here, half of the crown ether molecules coordinate to a thallium(I) cation. As is typical for many Tl-18c6 compounds, Tl(I) is found in the so-called “sunrise conformation” above the crown ether. The reason for this unusual conformation has been recently explained.²⁵ The distance of the thallium cation

Table 4. Selected Interatomic Distances and Angles for $[(M@18c6)_2][TiL_4] \cdot 2H_2O$, $M = (H_3O, H_2O), (NH_4, NH_3)$, and Tl

[(Ti@18c6 ₂)[TiL ₄]·2 H ₂ O			
	<i>d</i> (pm)		∠ (deg)
O(1)–C(1)	1.414(7)	C(1)–O(1)–C(2)	112.7(5)
O(1)–C(2)	1.426(8)	O(1)–C(1)–C(2)	108.5(5)
C(1)–C(2)	1.502(9)	O(1)–C(2)–C(1)	108.2(5)
Tl(1)–I	2.7574(6)	O(1)–C(1)–C(2)–O(2)	70
Tl(2)–O(4)	0.76(5)	C(1)–O(1)–C(2)–C(1)	178
Tl(2)–Ti(2)	2.692(4)	C(2)–O(1)–C(1)–C(2)	180
[(NH ₄ ,NH ₃)@18c6 ₂][TiL ₄]·2 H ₂ O			
	<i>d</i> (pm)		∠ (deg)
O(1)–C(1)	141.6(7)	C(1)–O(1)–C(2)	112.4(4)
O(1)–C(2)	143.1(7)	O(1)–C(1)–C(2)	108.7(5)
C(1)–C(2)	150.5(9)	O(1)–C(2)–C(1)	107.8(5)
Tl–I	275.82(6)	O(1)–C(1)–C(2)–O(2)	70
N–O(2)	0.65(2)	C(1)–O(1)–C(2)–C(1)	178
N–O(1)	305.8	C(2)–O(1)–C(1)–C(2)	179
O(2)–O(1)	336		
[(H ₃ O,H ₂ O)@18c6 ₂][TiL ₄]·2 H ₂ O			
	<i>d</i> (pm)		∠ (deg)
O(1)–C(1)	140.7(11)	C(1)–O(1)–C(2)	112.5(8)
O(1)–C(2)	143.5(12)	O(1)–C(1)–C(2)	108.6(9)
C(1)–C(2)	150.4(15)	O(1)–C(2)–C(1)	107.7(9)
Tl–I	276.10(9)	O(1)–C(1)–C(2)–O(2)	72
O(2)–O(2)	287	C(1)–O(1)–C(2)–C(1)	179
		C(2)–O(1)–C(1)–C(2)	178

to the least-squares plane of the crown ether is 134(1) pm, and the distances toward the crown ether oxygen atoms are 304.1 and 321.6 pm. For comparison, the Tl⁺ ion in $[Ti(18c6)_4CuCl_4][TiCl_4]_2 \cdot 0.25 H_2O$ ¹ is found to reside 92 pm above the least-squares plane of the six crown ether oxygen atoms with Tl–O distances of 294.1 pm and 304.6 pm. In the isomorphous $[Ti(18c6)_4CuBr_4][TiBr_4]_2$,² Tl–O distances of 291 pm and 311 pm are observed with the Tl⁺ cation, 110 pm above the crown. In $[Ti(18c6)_4MnCl_4][TiCl_4]_2$,³ the Tl–O distances are 293 pm and 301 pm, and the Tl cation is found 93 pm above the least-squares plane of the crown ether oxygen atoms. The crystal water molecules in $[Ti(18c6)_2][TiL_4] \cdot 2H_2O$ are disordered over eight corners of a distorted cube inside a tetrahedron spanned by the crown ether molecules. As an occupancy of one-quarter is found for the oxygen positions of the crystal water, only two corners of the cube are statistically occupied. These oxygen atoms have an interatomic distance of 274(3) pm.

The question of how the guest structures can adjust to accommodate (host) negatively charged transition metal units remains. Our investigations show that there are two principal ways. In case of the thallium compound, upon incorporation of the $[MX_4]^{2-}$ units, solvent water (previously complexed by the crown ether) is replaced by additional thallium(I) cations. The transformation in case of the (NH_4^+, NH_3) and the (H_3O^+, H_2O) compound is easier because additional protonation of the complexed ammonia and water is all that is needed to compensate for the extra charge.

Interestingly, all of these cubic host compounds, $[(M@18c6)_2][TiL_4] \cdot 2H_2O$, $M = (NH_4, NH_3)$ and Tl, can be obtained only in the presence of traces of transition metals

(25) Mudring, A.-V.; Rieger, F. *Inorg. Chem.* **2005**, *44*, 6240.

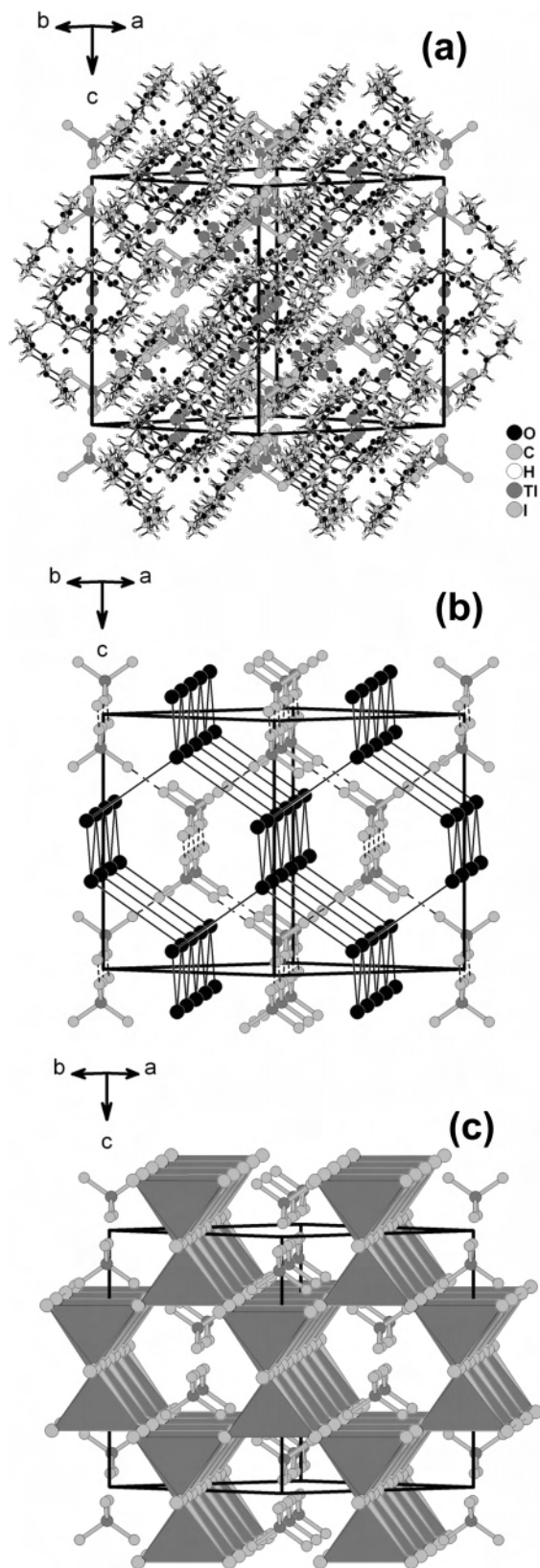


Figure 5. Crystal structure of $[\text{Ti}(\text{18c6})_2][\text{TiI}_4] \cdot 2\text{H}_2\text{O}$ showing the (a) view along $[110]$ (b) Two interpenetrating diamond-like nets formed by the $[\text{TiI}_4]^-$ units (connections in dotted lines) and the centers of gravity of four tetrahedrally arranged 18c6 molecules (black circles, connections in straight black lines) resulting in a NaTi -like structure. Crown ether and crystal water molecules as well as 18c6-coordinated $\text{Ti}(\text{I})$ are omitted for clarity. (c) MgCu_2 -like arrangement of $[\text{TiI}_4]^-$ ions and the 18c6 centers (edge-linked medium gray closed tetrahedra).

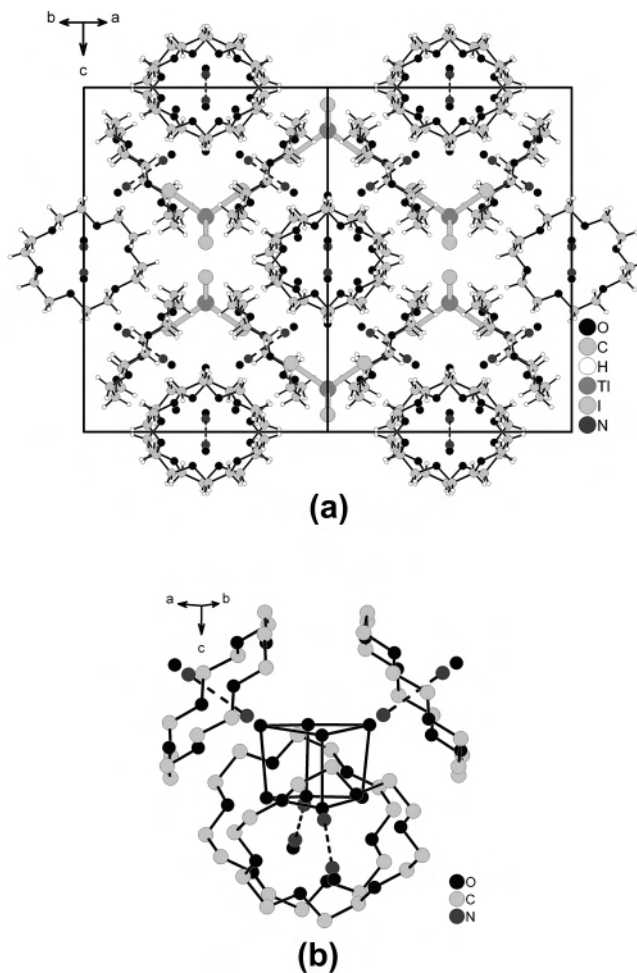


Figure 6. (a) View of the crystal structure along $[110]$ and (b) disorder among $(\text{NH}_4/\text{NH}_3)$ and solvent water in $[(\text{NH}_4/\text{NH}_3)@18\text{c6}]_2 \cdot [\text{TiI}_4] \cdot 2\text{H}_2\text{O}$.

(like copper and mercury halides in our investigations). Otherwise simple compounds such as $[\text{Ti} @ 18\text{c6}][\text{TiI}_4]^{25}$ are formed. Although the transition metals are never found in the crystal structure (no electron density is observed in the middle of the tetrahedra formed by the crown ether molecules where the $[\text{M}^{\text{II}}\text{X}_4]$ moieties are located in the host–guest compounds), the small amounts present in the solution must have a structure directing effect, most probably by forming tetrahedral $[\text{MX}_4]$ units with the halide anion present in the reaction mixture as found in the $[(\text{M}^{\text{II}}\text{X}_4)(\text{M}^{\text{I}} @ 18\text{c6})_4][\text{TiX}_4]_2 \cdot n\text{H}_2\text{O}$ ($\text{M}^{\text{II}} = \text{Cu}, \text{Co}, \text{Zn}, \text{Mn}$; $\text{M}^{\text{I}} = \text{NH}_4^+, \text{Rb}, \text{TI}$; $\text{X} = \text{Cl}, \text{Br}$) host–guest complexes.^{1–5} In this sense, the transition metal tetrahedra would work as a template. A first shell of crown ether molecules wraps around them and a second, adamantane-like shell of $[\text{TiI}_4]$ tetrahedra is subsequently built up. After the initial $[\text{MX}_4]$ units leave the cavity, crystal water is incorporated to stabilize the open structure.

Thus, the compounds under investigation are not only host lattices for tetrahedrally coordinated transition metal units as already proven by the large group of $[(\text{M}^{\text{II}}\text{X}_4)(\text{M}^{\text{I}} @ 18\text{c6})_4][\text{TiX}_4]_2 \cdot n\text{H}_2\text{O}$ ($\text{M}^{\text{II}} = \text{Cu}, \text{Co}, \text{Zn}, \text{Mn}$; $\text{M}^{\text{I}} = \text{NH}_4^+, \text{Rb}, \text{TI}$; $\text{X} = \text{Cl}, \text{Br}$)^{1–5} host–guest complex compounds but also show that crystal engineering can be accomplished by tetrahedrally coordinated transition metal units.

Acknowledgment. The Deutsche Forschungsgemeinschaft and the Fonds der Chemischen Industrie (Liebig fellowship to A.V.M.) are acknowledged for generous financial support. The authors would like to thank Prof. Dr. Gerd Meyer, Universität zu Köln, for his helpful comments.

Supporting Information Available: Crystallographic data files in CIF format. This material is available free of charge via the Internet at <http://pubs.acs.org>.

IC051430Z